Organic chemistry |Hot Paper|

π-Extended Diaza[7]helicenes by Hybridization of Naphthalene Diimides and Hexa-*peri*-hexabenzocoronenes

Carolin Dusold,[a] Dmitry I. Sharapa,[b] Frank Hampel,[a] and Andreas Hirsch*[a]

Abstract: The synthesis of an unprecedented, π-extended hexabenzocorene (HBC)-based diaza[7]helicene is presented. The target compound was synthesized by an *ortho*-fusion of two naphthalene diimide (NDI) units to a HBC-skeleton. A combination of Diels–Alder and Scholl-type oxidation reactions involving a symmetric di-NDI-tolane precursor were crucial for the very selective formation of the helical superstructure via a hexaphenyl-benzene (HPB) derivative. The formation of the diaza[7]helicene moiety in the final Scholl oxidation is favoured, affording the symmetric π-extended helicene as the major product as a pair of enantiomers. The separation of the enantiomers was successfully accomplished by HPLC involving a chiral stationary phase. The absolute configuration of the enantiomers was assigned by comparison of circular dichroism spectra with quantum mechanical calculations.

Introduction

The development of nonplanar PAHs is currently an emerging field in synthetic organic chemistry.[1] Among the most important starting points for this progress is the discovery of the parent helicenes.[2] Since then, research groups all over the world further elaborated the investigation and understanding of helicene chemistry, with great success.[3] Outstanding chiroptical properties,[4] such as inducing the emission of circularly polarized light, large optical rotation values and pronounced circular dichroism bands make them very attractive for applications in nonlinear optics,[5] asymmetric synthesis,[6] chiroptical switches,[7] and organic semiconductors.[8] Next to the classical carbohelicenes, heterohelicenes, which include one or more heteroaromatic rings such as pyridine, pyrrole, and thiophene are receiving growing interest and it was realized that their property combinations can even surpass those of the conventional all-carbon analogues.[9] Furthermore, the π-extension of the basic helicene skeleton is of considerable interest since it can notably tune optical, electronical and supramolecular properties.[10] Elongation of the spiral arrangement of the conjugated π-system represents the most common way to prepare higher helicene derivatives.[11] In contrast to that, the expansion of the conjugated system on the outer rim is still a challenging issue. Recently, a lot of progress has been made on the lateral extension of helicenes,[10a,12] including π-extended helicenes based on perylene diimide,[13] pyrene[14] and hexa-*peri*-hexabenzocoronene (HBC).[15] Especially the use of HBC subunits enables the design of new „superhelicenes“,[15a] representing new proto-types in the field of chiral nanographene. Such helically twisted graphenes can be considered as promising candidates in the field of chiral electronics,[16] not only due to their outstanding chiroptical properties, but also due to an enhanced π–π stacking relative to the parent helicene, which is crucial to achieve efficient charge carrier transportation,[17] and an improved solubility compared to their planar analogues.[18] In this contribution, we will expand the concept of HBC-based helicenes by introducing additional aromatic subunits to further extend the conjugated π-system. We have selected naphthalene diimides (NDIs) as promising candidates since they feature desirable chemical and (opto)electronical properties themselves.[19] As a consequence, we accomplished an *ortho*-fusion of two NDI units to an HBC-skeleton, generating an unprecedented, π-extended HBC-based heterohelicene. The high degree of pre-organization of the diaza[7]helicene subunit results in the formation of a chiral compound with two NDI arms lying on top of each other (Figure 1).

This helical superstructure combines not only the advantages of lateral π-extended helicenes with those of azahelicenes, at the same time, the fusion of two NDI arms enables the generation of an extensive conjugated π-surface all over the molecule. Photophysical investigations were carried out and the corresponding enantiomers were separated in order to determine their chiroptical properties.

[a] C. Dusold, Dr. F. Hampel, Prof. Dr. A. Hirsch
Department of Chemistry and Pharmacy
Friedrich-Alexander University Erlangen-Nürnberg
Nikolaus-Fiebiger-Straße 10, 91058 Erlangen (Germany)
E-mail: andreas.hirsch@fau.de

[b] Dr. D. I. Sharapa
Institute of Catalysis Research and Technology
Karlsruhe Institute of Technology
Hermann-von-Helmholtz-Platz 1, 76344 Eggenstein-Leopoldshafen (Germany)

Supporting Information and the ORCID identification number(s) for the author(s) of this article can be found under:
https://doi.org/10.1002/chem.202003402.

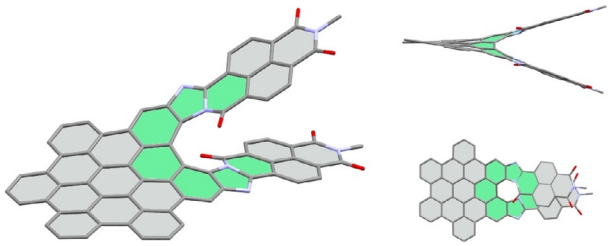

Figure 1. General structure of a chiral, π-extended diaza[7]helicene based on HBC and NDI.

Results and Discussion

Our strategy to synthesise the π-extended HBC-based diaza[7]-helicene HBC **3** relies on the combination of standard Diels–Alder and Scholl-type reactions (Scheme 1).

The key intermediate of our synthetic concept is the tolane derivative **1** containing two symmetrically fused NDI units. The symmetric constitution of the corresponding di-NDI-hexaphenyl-benzene (HPB) (**2**) is crucial to generate the desired 7-helical moiety in the final HBC. The synthetic sequence started with the preparation of the symmetric precursor **1** as illustrated in Scheme 2.

The first step was the palladium-catalysed Sonogashira cross-coupling reaction between *tert*-butyloxycarbonyl (boc)-protected alkyne **4** and 4-bromo-1,2-naphthaleneimidebenzimidazole (**5**). The required boc-protected alkyne building block **4** was prepared according to literature procedures,[20] starting with the protection of diamino-bromobenzene (**11**) to enable the successful performance of the subsequent Sonogashira coupling reactions, followed by deprotection of the TMS-group (see Supporting Information S1 for synthetic details). The second building block NDI-compound **5** was prepared via condensation of naphthalene monoimide (**8**) with diamino-bromobenzene (**11**) (Scheme 3). During this reaction, two constitutional isomers are formed, **5** as well as 5-bromo-1,2-naphthaleneimidebenzimidazole (**12**). The two compounds can easily be separated by column chromatography, isolating the first yellow fraction in 42% yield, and the second orange fraction in 36% yield. Although the NMR and optical spectra of both compounds differ significantly as shown in Scheme 3 (for further information see Supporting Information S2), clear structural assignment was not possible at this point. However, crystals of the orange fraction suitable for X-ray diffraction analysis were grown by slow evaporation of a solution of the compound in dichloromethane (DCM) at room temperature. Small needles were obtained, and the quality of the X-ray analysis was sufficient for unambiguous structure assignment (see Supporting Information S2 for further information). Thus, a secure assignment of the orange fraction to the **5** isomer is possible as depicted in Figure 2.

The boc-protected NDI-tolane **6** synthesised by Sonogashira reaction was obtained in a pure form in good yields of 82% (Scheme 2). The boc-protecting group was removed using TFA[21] to afford the free diamino functionality. Due to the sensitivity towards oxidation of such aminotolane compounds,[22] the crude product **7** was used directly in the next condensation reaction with **8** without further purification or characterisation to generate di-NDI-tolane precursors **1** and **9** with an overall yield of 56%. The new fused naphthalene benzimidazole moiety is once again formed as two constitutional isomers. One the one hand, a symmetrical compound **1** is formed in which the introduced naphthalene monoimide is connected to the tolane in a binding pattern similar to the already existing naphthalene-benzimidazole unit, highlighted in blue in Scheme 2. On the other hand, an asymmetric tolane is formed when the naphthalene monoimide is fused to the tolane in an alternative binding pattern, highlighted in red. The asymmetric tolane **9** is not a suitable precursor for the targeted π-extended HBC-based diaza[7]helicene HBC **3**, since planarization of the corresponding asymmetrical HPB **10** would not result in the desired 7-helical structure in the end. The symmetrical di-NDI tolane **1** with both NDI units fused to it through the blue binding pattern is essential for the formation of the helical superstructure in the final compound. Unfortunately, isomers **1** and **9** could not be separated at this stage. Hence, the fused di-NDI-tolane was reacted as a mixture of isomers in the subsequent Diels–Alder reaction with tetrakis-(*tert*-butyl)tetracyclone[15a,23] at 220 °C to generate the corresponding di-NDI HPBs **2**

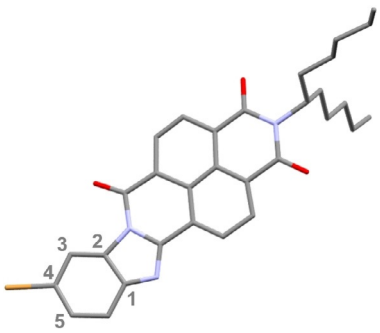

Figure 2. Crystal structure of 4-bromo-1,2-naphthaleneimidebenzimidazole (**5**).

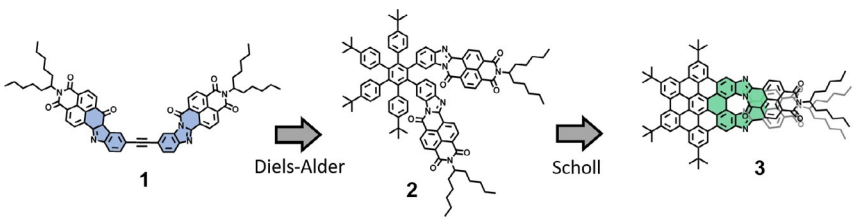

Scheme 1. Synthetic concept to generate 7-helical HBC **3**.

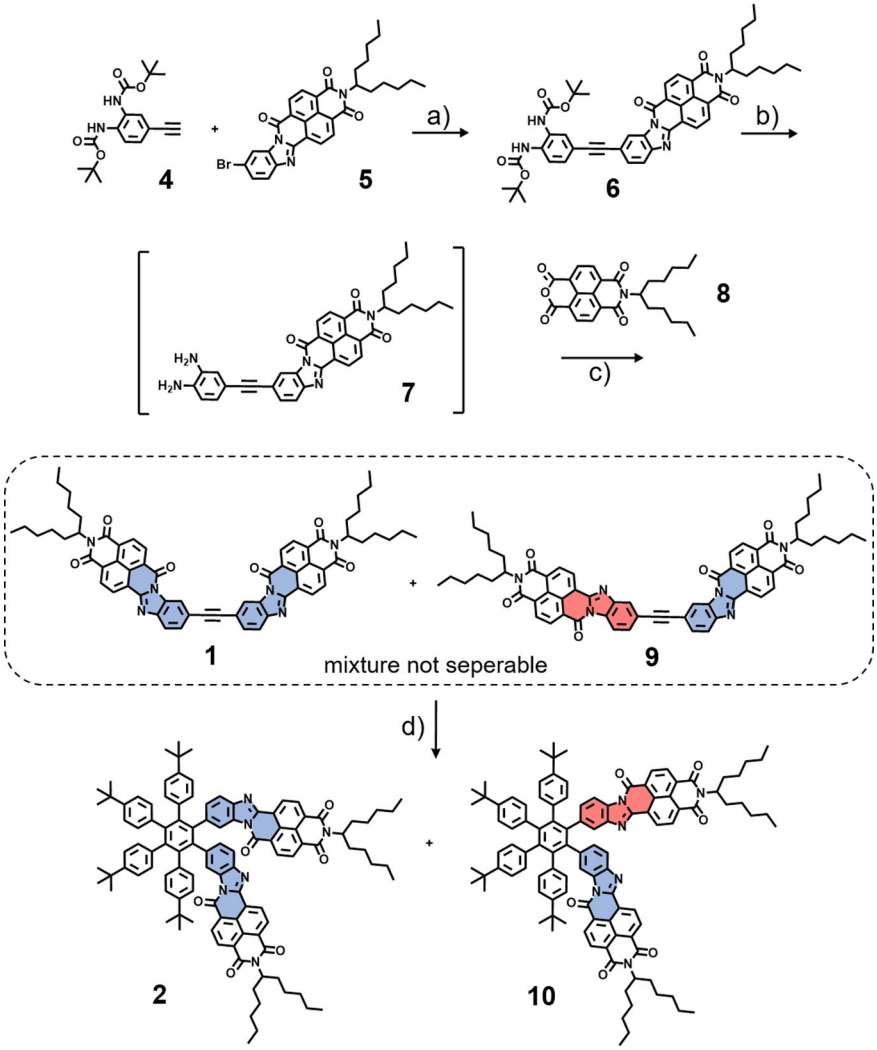

Scheme 2. Synthesis of symmetric and asymmetric di-NDI HPBs **2** and **10**. a) $PdCl_2(PPh_3)_2$, CuI, Et_3N, toluene, 80 °C, 18 h, yield 82 %. b) TFA, DCM, RT, 3 h. c) DMF, 140 °C, 18 h, yield 56 %. d) Tetrakis-(*tert*-butyl)tetracyclone, toluene, 220 °C, 24 h, yield 29 % (**2**) and 30 % (**10**).

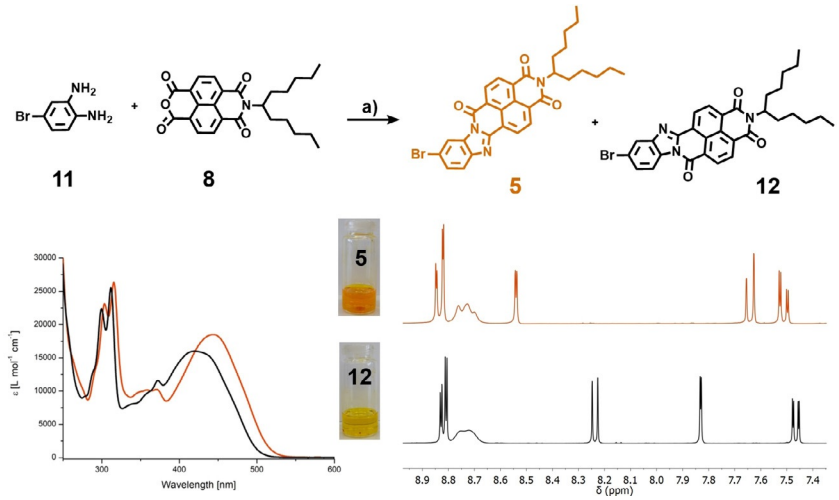

Scheme 3. Synthesis of the naphthalene imide benzimidazole isomers **5** (orange) and **12** (black) and their ^{1}H NMR and UV/Vis absorption spectra. a) Imidazole, 160 °C, 3 h, yield 36 % (**5**) and 42 % (**12**).

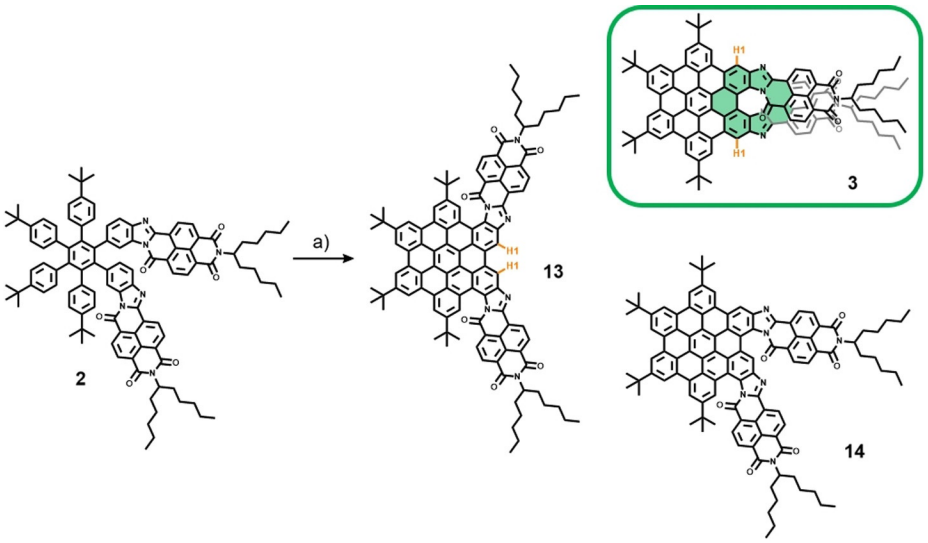

Scheme 4. Final Scholl-oxidation of HPB **2** leading to the three possible isomers symmetrical HBC **13**, 7-helical HBC **3**, and asymmetrical HBC **14**; hydrogen atoms without COSY-correlation: H1 highlighted in orange a) $FeCl_3$, CH_3NO_2, DCM, 0 °C, o.n. (overnight), yield 43 %.

and **10**. At this stage the two isomers could easily be separated by column chromatography in pure form. Symmetrical HPB **2** was obtained in 29 % and asymmetrical HPB **10** in 30 % yield. For the final transformation of di-NDI HPB **2** Scholl oxidation conditions using $FeCl_3$ were applied. After 18 h, complete conversation of the starting material was observed, and new dark-green compounds were traced by TLC. The crude mixture was separated by HPLC (see Supporting Information S3). Next to the expected molecules **3**, **13** and **14** several minor side-products were detected, in particular chlorinated side-products as well as compounds with one bond of the HBC core still not closed. However, the major fraction of the reaction was identified as the product by mass spectrometry. In Scheme 4, the structure of the three constitutional isomers formed during the final Scholl oxidation, namely, the two symmetrical isomers **13** and **3** and the asymmetrical isomer **14** is depicted.

HPLC separation resulted in exclusive isolation of fraction **3**, which was analysed by NMR spectroscopy. The important regions of the proton ^{1}H NMR spectrum are displayed in Figure 3. The spectrum reveals a defined set of signals, already indicating the existence of one pure compound instead of a mixture of isomers. In the aromatic area five signals for the protons of the HBC are present between 9.32–10.03 ppm and four signals between 8.19–9.06 ppm that can be assigned to the NDI hydrogen atoms. Moreover, only one resonance can be found at 4.92 ppm (N-CH) and the protons of the *tert*-butyl groups of the HBC unit appear as only two singlets at 1.85 and 1.80 ppm. The appearance of only one set of resonances suggest that the isolated compound must be symmetrical, which is consistent with either the desired 7-helical HBC **3** or HBC **13**.

For an unambiguous structural assignment, additional 1D and 2D NMR experiments were performed (see Supporting Information S4). The ^{1}H-COSY-NMR spectrum exhibits the coupling of the aromatic hydrogen atoms, except for the HBC protons at 10.03 ppm, which features no such correlation. This characteristic is in principle still compatible for hydrogen atoms H1 (highlighted in orange) for both symmetrical isomers (Scheme 4). However, 1D-ROESY NMR spectroscopy shows that selective excitation of this resonance at 10.03 ppm results in a strong signal at 9.58 ppm. Since hydrogen atoms H1 of HBC **13** are completely isolated, no NOE (nuclear Overhauser effect) signal is expected, unlike the H atoms H1 of HBC **3**, which exhibit neighbouring protons at the HBC-rim. Thus, this is a first indication that the isolated fraction is the desired, isometrically pure diaza[7]helicene HBC **3**. Hence, Scholl oxidation of symmetric di-NDI HPB **2** favours the formation of the 7-helical structure. One possible explanation for this could be the π–π interaction of the two NDI units that is most pronounced once they lie on top of each other causing a suitable pre-orientation of the HPB. As a result, 7-helical HBC **3** is formed as the major compound which was isolated in 43 % yield. HBC **13** and **14** were formed only in minor quantities (< 1 mg) and could not be isolated. The structural assignment is supported by a very

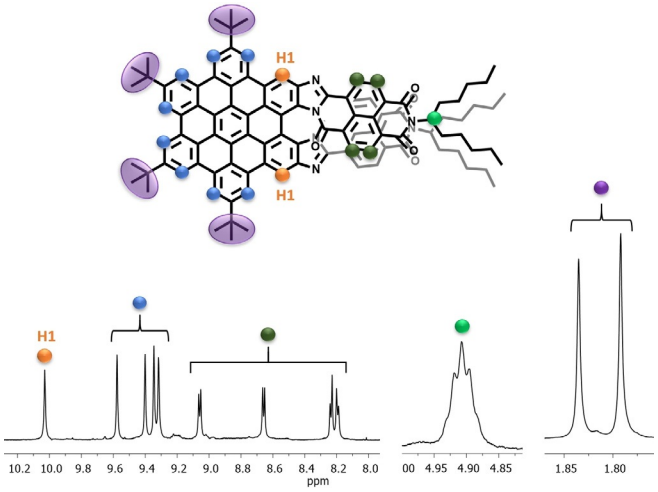

Figure 3. Important regions of the ^{1}H-NMR spectrum of 7-helical HBC **3**.

good resolution of all NMR spectra of HBC **3**, which were recorded at room without the necessity to perform high-temperature measurements. It is expected that such extended aromatic systems form intermolecular aggregates due to strong π–π interactions, which would drastically decrease the solubility. Thus, compound **13** should not be resolvable at room temperature. However, the nonplanar helicene subunit and the inherent three-dimensional twist of HBC **3** provides excellent solubility in a very large variety of organic solvents. In comparison, the symmetrical HPB **2** shows a much lower solubility and thus, high-temperature NMR measurement were needed to obtain spectra with good resolution (see Supporting Information S5). The transformation of di-NDI-HPB **2** to the corresponding HBC **3** can be monitored by UV/Vis absorption spectroscopy as well (Figure 4). After Scholl oxidation, HCB **2** displays a new strong absorption signature due to the HBC unit at 372 nm with a high molar extinction coefficient of 54000 $L mol^{-1} cm^{-1}$. At the same time, the NDI absorption broadens and experiences a strong red shift of 100 nm to 571 nm. In addition, the intensity decreases from extinction coefficient values of around 25000 to 11100 $L mol^{-1} cm^{-1}$.

Emission properties were investigated upon irradiation at the corresponding absorption maximum. Although the starting material **5** exhibits a very strong fluorescence with a maximum at 570 nm, the emission intensity is already drastically decreased for di-NDI tolane mixture **1**/**9** as well as for HPB **2**. Finally, the fluorescence of the 7-helical HBC **3** is completely quenched, and no emission is detected any more (see Supporting Information S6).

Since compound **3** contains a diaza[7]helicene unit, it is a chiral molecule and can adopt either (M)- or (P)-configuration (Figure 5 A). In order to separate the enantiomers, we targeted HPLC using a chiral Chiralpak 1BN-5 column. Indeed, we were able to separate the two enantiomers with retention times of $t_R = 14.7$ min and $t_R = 31.3$ min. This allowed us to analyse their chiroptical properties with circular dichroism (CD) spectroscopy (Figure 5 B + C). The mirror image spectra display five strong Cotton effects in the ultraviolet and visible region between 260–340 nm, 365–390 nm, 390–430 nm, 430–460 nm and 580–730 nm with corresponding $|\Delta\varepsilon|$ of 33, 25, 16, 15 and 10 $L mol^{-1} cm^{-1}$, respectively. The calculated dissymmetry factors $|g_{abs}|$ reach a maximum of 1.5×10^{-3}. In addition, we conducted DFT calculations (Figure 6) to gain information about the 3D-structure of **3**.

Traditionally, π–π stacking is better described by dispersion-corrected than by dispersion-devoid DFT. However, there are some works claiming that in condensed phase the uncorrected approach might be more consistent with reality.[24] Thus, we performed optimisation both with B3LYP/def2-SVP (Figure 6) and B3LYP-D3/def2-SVP (Figure S28) and for both geometries CD-spectra were simulated with same methodology (sTD-CAM-B3LYP/def2-TZVP, see S7 + S8 for details). Although the electronic structure (Figure 6 D) is very consistent for both obtained geometries (the highest occupied molecular orbital (HOMO) is mainly delocalized on the HBC unit while the lowest unoccupied molecular orbital (LUMO) is equally localized on both NDI moieties), the obtained geometries differ significantly in the interplanar distance of the two NDI-wings. This indeed shifts and effects the intensity of peaks in the long-wave part of the CD-spectra that corresponds to excitations with significant role of the LUMO. Nevertheless, the general pattern of the spectra stays the same for both geometries and is in good agreement with the experimentally measured spectra (especially in the area between 350–500 nm, see Figure 5 C). Thus, the first eluted fraction was assigned as (M)- and the second eluted fraction as (P)-isomer. Furthermore, characteristic helicity values such as torsion angles and interplanar angle, were analysed. The inner helix with corresponding torsion angles as well as the interplanar angle is shown in Figure 6 B and 6C, respectively. The seven rings form a helicene subunit with an overall sum of torsion angles α–ε of $\theta = 95°$–$106°$ (with and without dispersion correction). This value is between the ones of previously reported [7]-helicenes, for example, all carbon [7]-helicenes (sum of torsion angles 108° −134°)[3h,10a] or [7]-azahelicenes (sum of torsion angles 80.2°).[9a,25]

First titration experiments were performed to examine the efficiency of **3** to quench the emission of a fluorescent molecule and it was found that the emission intensity of anthracene

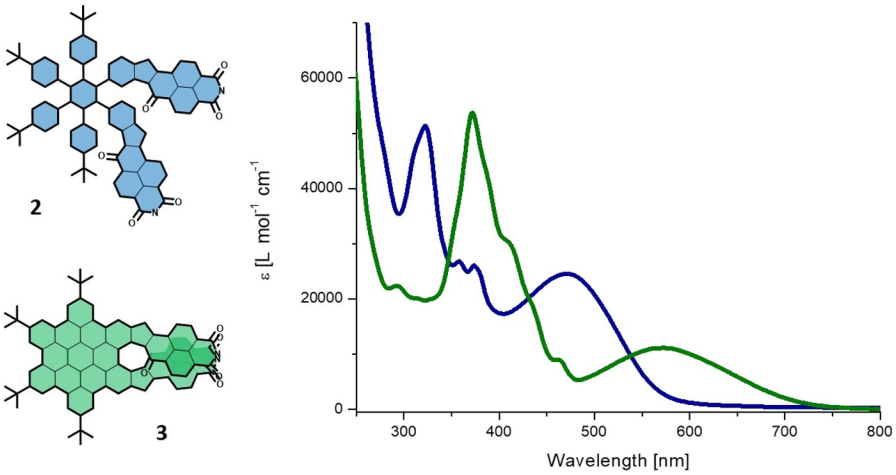

Figure 4. Comparison of UV/Vis absorption spectra of HPB **2** (blue) and 7-helical HBC **3** (green).

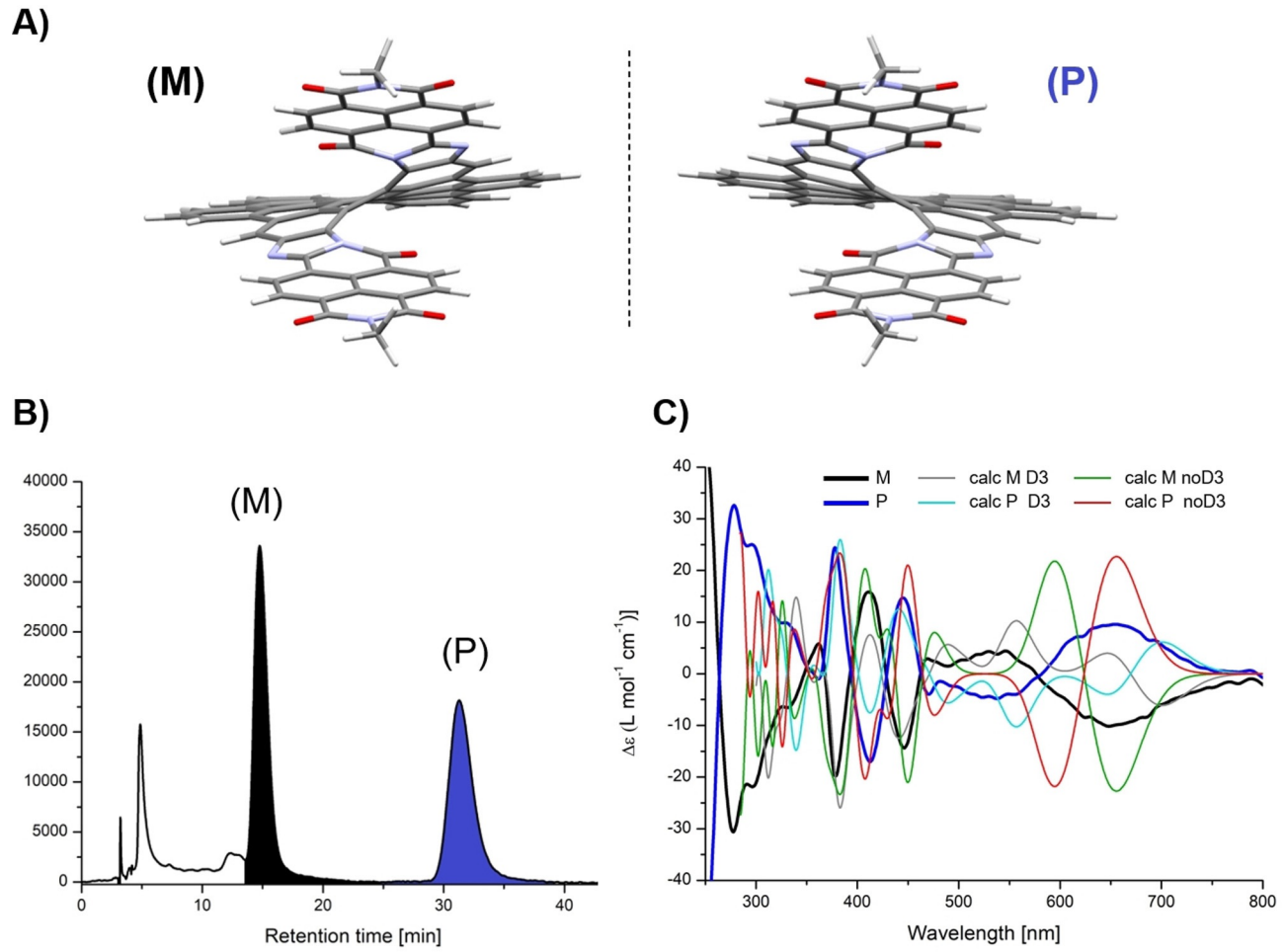

Figure 5. A) (M)- and (P)-configuration of 7-helcial HBC **3**, *t*Bu groups and swallow tail are omitted for clarity; B) chiral separation of **3** (Chiralpak 1BN-5, *n*-heptane/EtOH/diethylamine (DEA) 70:30:0.1, 4mLmin^{-1}, RT); C) CD spectroscopy measurements of (M)-**3** (black) and (P)-**3** (blue) and the corresponding calculated spectra (sTD-CAM-B3LYP/def2-TZVP with D3: grey, light blue; without D3 red, green).

significantly gets quenched after the successive addition of **3**. Theoretical calculations support the idea of anthracene being enclosed within the NDI units (see Supporting Information S9 for further information). The successful development of the synthetic strategy to HBC **3** opens up the access to a new compound class, which can be described as HBC based, chiral nano-tweezers having two structurally similar, π-extended ryleneimide arms. In this series, HBC **3** with its two NDI wings represents the smallest compound with promising structural features stemming from the high pre-organisation of the diaza[7]-helicene subunit. Using larger ryleneimides, to elongate the aromatic tweezer-arms, will further increase the cavity of such helical tweezers and, as a consequence, opens exciting opportunities for the supramolecular interaction with interdigitated host molecules.

Conclusions

Two naphthalene diimide (NDI) units were fused to a hexabenzocorene (HBC) through a benzimidazole bridge for the first time to generate a π-extended aza-helicene framework **3** that was investigated with respect to its photophysical and chiroptical properties. The *ortho*-fusion of the NDI units to the HBC leads to the formation of a fully conjugated diaza[7]helicene as a new helical hybrid involving a wide lateral π-extension of the helicene skeleton. During final Scholl oxidation, the 7-helical HBC **3** was the only product formed out of three possible isomers as pair of enantiomers, demonstrating pronounced stereoselectivity of the formation process. The enantiomers were separated by HPLC employing a chiral stationary phase. The chiroptical properties investigated with circular dichroism (CD) measurements were supported by theoretical calculations, which also allowed for an assignment of the absolute configuration of the isolated enantiomers. For a better understanding as to why a hexaphenyl-benzene (HPB) precursor is forced to adopt a 7-helical conformation and in order to prevent the formation of unwanted side products, improved synthetic protocols for the final Scholl oxidation are currently studied. The synthetic access to aza[*n*]helicenes such as **3** will pave the way for the exploration of unprecedent chiral nanotweezers with two rigid functional arms. The use of the higher ryleneimide analogues, in particular perylene-imides, to create a tweezer with even longer and more extended π-surface, is currently under investigation.

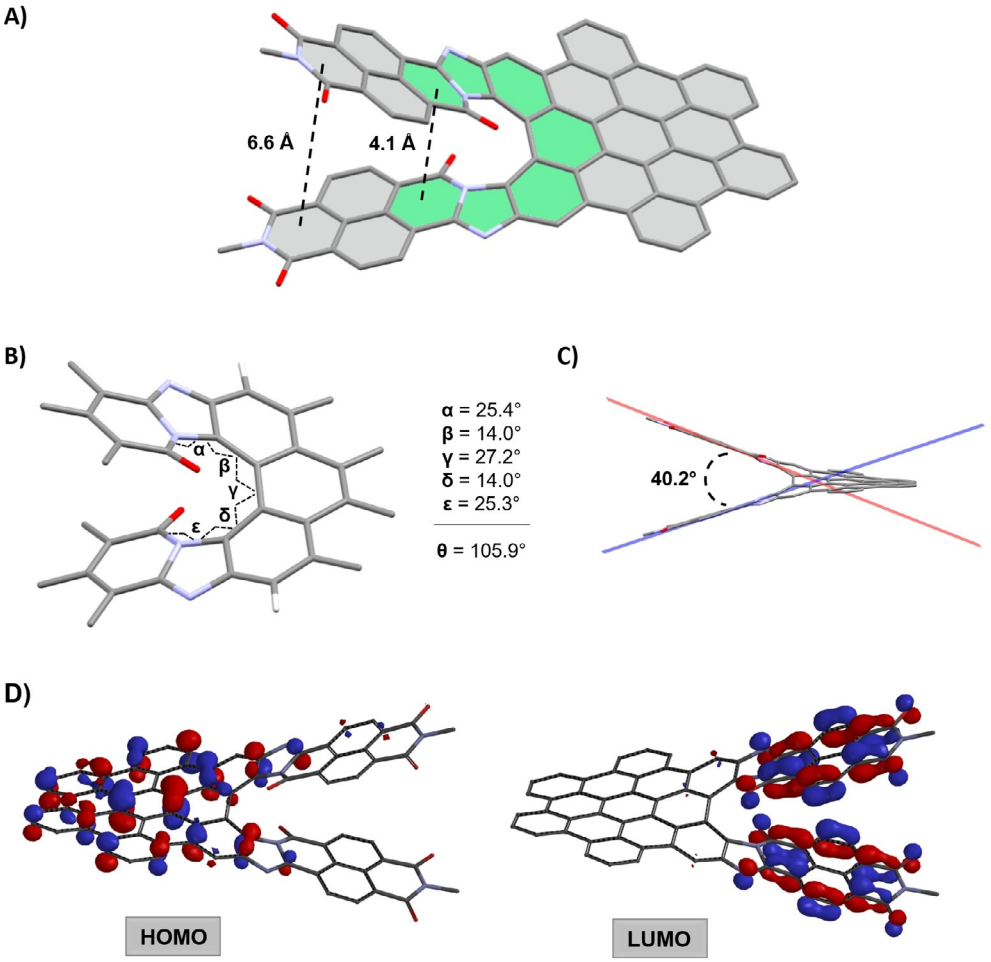

Figure 6. Geometry-optimised structures of HBC **3** at B3LYP/def2-SVP without dispersion correction; hydrogen atoms, *t*Bu groups and swallow tail are omitted for clarity; A) top view with relevant distances between the two NDI arms; B) torsion angles of the inner helix; C) side view with interplanar angle of the inner helix; D) representation of the highest occupied molecular orbital (HOMO) and the lowest unoccupied molecular orbital (LUMO).

Experimental Section

Chemicals were purchased from Sigma–Aldrich and used without any further purification. Solvents were distilled prior to usage. Thin layer chromatography (TLC) was performed on Merck silica gel 60 F524, detected by UV light (254 nm, 366 nm). Plug chromatography and column chromatography were performed on Macherey–Nagel silica gel 60 M (deactivated, 230–400 mesh, 0.04–0.063 mm). NMR spectra were recorded on a Bruker Avance 400 (^{1}H: 400 MHz, ^{13}C: 101 MHz), a Bruker Avance 500 (^{1}H: 500 MHz, ^{13}C: 126 MHz), or a Bruker Avance Neo Cryo-Probe DCH (^{1}H: 600 MHz, ^{13}C: 151 MHz). Deuterated solvents were purchased from Sigma–Aldrich and used as received. Chemical shifts are given in ppm at room temperature and are referenced to residual protic impurities in the solvents (^{1}H: $CHCl_3$: 7.24 ppm, $C_2H_2Cl_4$: 5.91 ppm) or the deuterated solvent itself ($^{13}C\{^{1}H\}$: $CDCl_3$: 77.16 ppm, $C_2D_2Cl_4$: 74.20 ppm). The resonance multiplicities are indicated as „s" (singlet), „bs" (broad singlet), „d" (doublet), „t" (triplet), „q" (quartet) and „m" (multiplet). Mass spectrometry was carried out with a Shimadzu AXIMA Confidence (MALDI-TOF, matrix: 2,5-dihydroxybenzoic acid DHB, *trans*-2-[3-(4-tert-butylphenyl)-2-methyl-2-propenyliden]malononitrile, DCTB) or without matrix (OM). High resolution mass spectrometry (HRMS) was recorded on a LDI/MALDI-ToF Bruker Ultraflex Extreme machine or on a APPI-ToF mass spectrometer Bruker maXis 4G UHR MS/MS spectrometer. UV/vis spectroscopy was carried out on a Varian Cary 5000 UV-vis-NIR spectrometer. The spectra were recorded at rt in DCM in quartz cuvettes (edge length = 1 cm) under ambient conditions. Fluorescence spectra were obtained from a Shimadzu RF-5301 PC and a NanoLog spectrofluorometer (Horiba Scientific). Circular dichroism spectroscopy was measured at rt in DCM on a Jasco J-815 spectrometer. HPLC separation was carried out using Shimadzu analytical and preparative HPLC with system controller CBM-20A, solvent delivery unit LC-20A, autosampler SIL-20A, column oven CTO-20A, photodiode array detector SPDM20A, on-line degassing unit DGU-20A and low-pressure gradient unit. All chromatograms were processed with Shimadzu LabSolution(c) software and exported as ASCII files.

4/5-Bromo-1,2-naphthaleneimidebenzimidazole (5) and (12): A dry flask was charged with NMI **8** (100 mg, 0.237 mmol, 1.1 equiv), 4-bromo-1,2-diaminbenzene **11** (40.0 mg, 0.216 mmol, 1 equiv) and imidazole (800 mg) and the mixture was stirred under nitrogen at 160 °C for 3 h. The reaction mixture was cooled to rt, diluted in DCM and washed with H_2O. The combined organic layers were concentrated under reduced pressure and the crude was purified by silica gel column chromatography (SiO_2, DCM/hexanes 1:1) to provide the two separated isomers **5** and **12** in a pure form. Yields: **5** (44.0 mg, 0.077 mmol, 36%), **12** (52.0 mg, 0.091 mmol, 42%).

4-Bromo-1,2-naphthaleneimidebenzimidazole (5): ^{1}H NMR ($CDCl_3$, 400 MHz, 25 °C): δ = 8.87–8.66 (m, 4H, Ar–CH), 8.54 (d, J = 1.8 Hz, 1H, Ar–CH), 7.64 (d, J = 8.6 Hz, 1H, Ar–CH), 7.51 (dd, J = 8.6, 1.9 Hz, 1H, Ar–CH), 5.37–5.01 (m, 1H, N–CH), 2.29–2.17 (m, 2H, CH_2), 1.96–1.67 (m, 2H, CH_2), 1.42–1.05 (m, 12H, CH_2), 0.92–0.68 (m, 6H, CH_3) ppm; ^{13}C NMR ($CDCl_3$, 101 MHz 25 °C): δ = 159.3 (C=O), 148.3, 143.0, 132.9 (Ar–C), 131.6, 130.0 (Ar–CH), 127.7 (Ar–C), 127.1 (Ar–CH), 126.9, 125.9, 125.1 (Ar–C), 121.9 (Ar–CH), 120.5 (Ar–C), 119.1 (Ar–CH), 55.4 (N–CH), 32.4, 31.8, 26.8, 22.7 (CH_2), 14.2 (CH_3) ppm; MS (MALDI-TOF, dctb): m/z = 572.2 (100%, $C_{31}H_{31}BrN_3O_3$ [M+H]$^+$); HRMS (APPI, CH_2Cl_2): calculated for $C_{31}H_{31}BrN_3O_3$ ([M+H]$^+$) m/z = 572.1543, found m/z = 572.1545; UV/Vis (CH_2Cl_2): λ [nm] (ε [L mol^{-1} cm^{-1}]) = 304 (23500), 316 (26500), 443 (18500); Fluorescence (CH_2Cl_2): $\lambda_{exc.}$ [nm] = 443, $\lambda_{emission}$ [nm] (rel. int.) = 570 (100).

5-Bromo-1,2-naphthaleneimidebenzimidazole (12): ^{1}H NMR ($CDCl_3$, 400 MHz, 25 °C): δ = 8.97–8.56 (m, 4H, Ar–CH), 8.24 (d, J = 8.5 Hz, 1H, Ar–CH), 7.83 (d, J = 1.8 Hz, 1H, Ar–CH), 7.47 (dd, J = 8.7, 1.8 Hz, 1H, Ar–CH), 5.33–4.98 (m, 1H, N–CH), 2.34–2.11 (m, 2H, CH_2), 2.05–1.69 (m, 2H, CH_2), 1.41–0.96 (m, 12H, CH_2), 0.93–0.51 (m, 6H, CH_3) ppm; ^{13}C NMR ($CDCl_3$, 101 MHz 25 °C): δ = 159.1 (C=O), 148.8, 145.2 (Ar–C), 131.6 (Ar–CH), 130.9 (Ar–C), 129.8 (Ar–CH), 127.6 (Ar–C), 127.2 (Ar–CH), 126.8, 125.8, 124.8 (Ar–C), 123.7 (Ar–CH), 119.7 (Ar–C), 116.9 (Ar–CH), 55.4 (N–CH), 32.4, 31.8, 26.8, 22.7 (CH_2), 14.2 (CH_3) ppm; MS (MALDI-TOF, dctb): m/z = 572.2 (100%, $C_{31}H_{31}BrN_3O_3$ [M+H]$^+$); HRMS (MALDI-TOF, dctb): calculated for $C_{31}H_{31}BrN_3O_3$ ([M+H]$^+$) m/z = 572.1543, found m/z = 572.1528; UV/Vis (CH_2Cl_2): λ [nm] (ε [L mol^{-1} cm^{-1}]) = 300 (22500), 312 (25500), 420 (16000); Fluorescence (CH_2Cl_2): $\lambda_{exc.}$ [nm] = 420, $\lambda_{emission}$ [nm] (rel. int.) = 556 (100).

NDI-Tolane (6): A 20 mL MW vial was charged with Br-Naph **5** (70 mg, 0.12 mmol, 1 equiv), $PdCl_2(PPh_3)_2$ (4.2 mg, 0.006 mmol, 0.05 equiv), CuI (0.5 mg, 0.003 mmol, 0.02 equiv) and toluene (4 mL) and sealed with a septum. The solution was degassed for 15 min and subsequently di-*tert*-butyl(4-ethynyl-1,2-phenylene)dicarbamate **4** (82.0 mg, 0.25 mmol, 2 equiv) dissolved in Et_3N (2 mL) was added via a syringe. The reaction mixture was stirred at 80 °C overnight under argon atmosphere. The solvent was removed under reduced pressure and the crude product was subjected to column chromatography (SiO_2; EtOAc/hexane 1:4) to provide the pure product **6** as a red solid (83 mg, 0.10 mmol, 82% yield). ^{1}H NMR ($CDCl_3$, 400 MHz, 25 °C): δ = 8.91–8.86 (m, 2H, Ar–CH), 8.75 (bs, 2H, Ar–CH), 8.61 (d, J = 1.5 Hz, 1H, Ar–CH), 7.79 (d, J = 8.4 Hz, 1H, Ar–CH), 7.69 (bs, 1H, Ar–CH), 7.59 (m, 2H, Ar–CH), 7.34 (dd, J = 8.4, 1.9 Hz, 1H, Ar–CH), 6.84 (bs, 1H, N–H), 6.66 (bs, 1H, N–H), 5.22–5.09 (m, 1H, N–CH), 2.28–2.13 (m, 2H, CH_2), 1.92–1.78 (m, 2H, CH_2), 1.53 (s, 9H, CH_3), 1.52 (s, 9H, CH_3), 1.35–1.18 (m, 12H, CH_2), 0.84–0.78 (m, 6H, CH_3) ppm; ^{13}C NMR ($CDCl_3$, 101 MHz 25 °C): δ = 159.3, 153.9, 153.5 (C=O), 148.7, 143.8, 132.1, 131.5, 130.3, 129.2, 127.8, 127.2, 126.9, 126.0, 125.3, 122.2, 120.8, 119.2 (Ar–CH, Ar–C), 90.6, 89.6 (C≡C), 81.4, 81.3 (C–CH_3), 55.4 (N–CH), 32.4, 31.9 (CH_2), 28.4 (CH_3), 26.8, 22.7 (CH_2), 14.2 (CH_3) ppm; MS (MALDI-TOF, dctb): m/z = 824.4 ($C_{49}H_{54}N_5O_7$ [M+H]$^+$); HRMS: (APPI, CH_2Cl_2) calculated for $C_{49}H_{54}N_5O_7$ ([M+H]$^+$) m/z = 824.4018 found m/z = 824.4011; UV/Vis (CH_2Cl_2): λ [nm] (ε [L mol^{-1} cm^{-1}]) = 328 (17100), 480 (6700).

Di-NDI-Tolane (1) and (9): Compound **6** (80.0 mg, 0.097 mmol, 1 equiv) was dissolved in DCM/trifluoroacetic acid (8 mL, 1:1 v/v) and stirred at room temperature for 3 h under nitrogen atmosphere.[21] Et_3N was added for neutralization and the mixture was filtered over silica. The solvent was removed under reduced pressure and due to the sensitivity towards oxidation of di-amino tolane **7**[22] the crude product was used in the next condensation reaction without further purification and characterization. Approximately 62 mg (0.100 mmol, 1 equiv) of the crude di-amino tolane **7** and naphthalene monoimide **8** (130 mg, 0.300 mmol, 3 equiv) were dissolved in DMF and heated to 140 °C for 18 h under argon atmosphere. The mixture was cooled to rt, extracted with DCM and washed with water. The solvent was removed under reduced pressure and the crude product was purified by plug chromatography (SiO_2; DCM) to provide the title compounds as an isomeric mixture **1** and **9** (54.0 mg, 0.054 mmol, 56% yield). MS (MALDI-TOF, dctb): m/z = 1009.5 (100%, $C_{64}H_{60}N_6O_6$ [M+H]$^+$); HRMS: (APPI, CH_2Cl_2/Tol): calculated for $C_{64}H_{60}N_6O_6$ ([M]$^+$) m/z = 1008.4569 found m/z = 1008.4595.

Di-NDI-HPB (2) and (10): A 1 mL MW-vial was charged with the isomeric mixture of di-NDI-tolanes **9** and **10** (54.0 mg, 0.054 mmol, 1 equiv), tetrakis-(*tert*-butyl)tetracyclone[15a,23] (50.0 mg, 0.081 mmol, 1.5 equiv) and toluene (1 mL) and sealed with a septum. The reaction mixture was degassed with N_2 for 5 min and heated to 220 °C for 24 h. The solvent was removed under reduced pressure and the crude was purified by column chromatography (SiO_2, THF/hexane 1:9) to provide the pure products **2** and **10**. Yields: symmetric di-NDI-HPB **2** (25.0 mg, 0.015 mmol, 29%), asymmetric di-NDI-HPB **10** (26.0 mg, 0.016 mmol, 30%).

Symmetric Di-NDI-HPB (2): ^{1}H NMR ($C_2D_2Cl_4$, 400 MHz, 135 °C): δ = 8.81–8.50 (m, 8H, Ar–CH), 8.14 (s, 2H, Ar–CH), 7.33 (d, J = 8.4, 2H, Ar–CH), 7.20–7.11 (m, 2H, Ar–CH), 6.93–6.66 (m, 16H, Ar–CH), 5.17–5.02 (m, 2H, N–CH), 2.24–2.12 (m, 4H, CH_2), 1.94–1.78 (m, 4H, CH_2), 1.39–1.19 (m, 24H, CH_2), 1.11 (s, 18H, CH_3), 1.00 (s, 18H, CH_3), 0.86–0.72 (m, 12H, CH_3) ppm; ^{13}C NMR ($C_2D_2Cl_4$, 101 MHz, 120 °C): δ = 158.9, 158.6 (C=O), 147.9, 147.7, 147.41, 147.36, 141.6, 141.5, 141.4, 141.1, 141.0, 140.7, 140.6, 139.3, 139.1, 137.7, 137.6, 137.4, 131.04, 130.99, 130.71, 130.67, 130.6, 127.50, 127.47, 127.4, 126.1, 125.7, 125.6, 125.5, 123.3, 123.1, 120.4, 119.4, 119.0, 118.7, (Ar-CH, Ar-C), 55.3 (N–CH), 34.0 (CH_2), 32.4 (C–CH_3), 31.7 (CH_2), 31.28, 31.20, 31.18 (CH_3), 26.6, 22.5 (CH_2), 14.0 (CH_3) ppm; MS (MALDI-TOF, dctb): m/z = 1589.9 (100%, $C_{108}H_{112}N_6O_6$ [M+H]$^+$); HRMS: (MALDI-TOF, dctb): calculated for $C_{108}H_{112}N_6O_6$ ([M]$^+$) m/z = 1588.8638 found m/z = 1588.8652; UV/Vis (CH_2Cl_2): λ [nm] (ε [L mol^{-1} cm^{-1}]) = 322 (51000), 471 (25000); Fluorescence (CH_2Cl_2): $\lambda_{exc.}$ [nm] = 471, $\lambda_{emission}$ [nm] (rel. int.) = 651 (100).

Asymmetric Di-NDI-HPB (10): ^{1}H NMR ($C_2D_2Cl_4$, 400 MHz, 135 °C): δ = 8.82–8.49 (m, 8H, Ar–CH), 8.13 (dd, J = 1.6, 0.7 Hz, 1H, Ar–CH), 7.94 (d, J = 8.4 Hz, 1H, Ar–CH), 7.53 (d, J = 1.4 Hz, 1H, Ar–CH), 7.34 (dd, J = 8.4, 0.7 Hz, 1H, Ar–CH), 7.22 (dd, J = 8.4, 0.8 Hz, 1H, Ar–CH), 7.13 (dd, J = 8.3, 1.6 Hz, 1H, Ar–CH), 6.89–6.71 (m, 16H, Ar–CH), 5.15–5.02 (m, 2H, N–CH), 2.20–2.10 (m, 4H, CH_2), 1.92–1.80 (m, 4H, CH_2), 1.34–1.20 (m, 24H, CH_2), 1.13–1.08 (m, 18H, CH_3), 1.02 (s, 9H, CH_3), 0.97 (s, 9H, CH_3), 0.84–0.76 (m, 12H, CH_3) ppm; ^{13}C NMR ($C_2D_2Cl_4$, 101 MHz, 120 °C): δ = 163.4, 163.2, 159.0 (C=O), 148.2, 148.1, 147.0, 147.9, 147.5, 147.4, 147.3, 146.0, 143.4, 141.9, 141.7, 141.6, 140.9, 140.8, 140.3, 140.2, 139.4, 139.2, 137.8, 137.7, 137.6, 131.3, 131.2, 130.6, 130.5, 129.8, 128.1, 128.0, 127.5, 127.4, 126.3, 125.8, 124.8, 124.8, 123.3, 123.2, 122.9, 118.8, 114.2, 113.7 (Ar–CH, Ar–C), 55.4 (N–CH), 34.0 (CH_2), 32.9 (C–CH_3), 31.4 (CH_2), 31.2 (CH_2), 31.20, 31.15, 31.09 (CH_3), 22.3 (CH_2), 13.7 (CH_3) ppm; MS (MALDI-TOF, dctb): m/z = 1590.1 (100%, $C_{108}H_{112}N_6O_6$ [M+H]$^+$); HRMS: (MALDI-TOF, dhb): calculated for $C_{108}H_{112}N_6O_6$ ([M]$^+$) m/z = 1588.8638 found m/z = 1588.8681; UV/Vis (CH_2Cl_2): λ [nm] (ε [L mol^{-1} cm^{-1}]) = 320 (37500), 450 (18000); Fluorescence (CH_2Cl_2): $\lambda_{exc.}$ [nm] = 451, $\lambda_{emission}$ [nm] (rel. int.) = 649 (100).

7-Helical HBC (3): In a 20 mL MW-vial symmetrical di-NDI-HPB **2** (20.0 mg, 12.6 μmol, 1 equiv) was dissolved in DCM (20 mL) and cooled to 0 °C with an ice bath. After degassing with N_2 for 20 min a solution of dry $FeCl_3$ (120 mg, 0.378 mmol, 60 equiv) in $MeNO_2$ (0.1 mL) was added. The mixture was degassed for further 15 min and stirred overnight. The reaction was quenched via the addition of MeOH. The solvent was removed under reduced pressure and the crude product was purified by HPLC chromatography to provide the pure product **3** as a dark green solid (8.2 mg, 5.2 μmol, 43 %). ^{1}H NMR ($C_2D_2Cl_4$, 600 MHz, 25 °C): δ = 10.03 (s, 2H, Ar–CH_{Cor}), 9.58 (s, 2H, Ar–CH_{Cor}), 9.40 (s, 2H, Ar–CH_{Cor}), 9.35 (s, 2H, Ar–CH_{Cor}), 9.32 (s, 2H, Ar–CH_{Cor}), 9.06 (d, J = 7.6 Hz, 2H, Ar–CH_{Naph}), 8.66 (d, J = 7.6 Hz, 2H, Ar–CH_{Naph}), 8.24 (d, J = 7.1 Hz, 2H, Ar–CH_{Naph}), 8.19 (d, J = 7.5 Hz, 2H, Ar–CH_{Naph}), 4.97–4.85 (m, 2H, N–CH), 2.28–2.17 (m, 4H, CH_2), 2.00–1.92 (m, 4H, CH_2), 1.84 (s, 18H, CH_3), 1.79 (s, 18H, CH_3), 1.28–1.10 (m, 24H, CH_2), 0.79–0.71 (m, 12H, CH_3) ppm; ^{13}C NMR ($C_2D_2Cl_4$, 151 MHz, 25 °C): δ = 156.8, 150.52 150.4, 149.7, 144.2, 130.9, 130.8, 130.7, 130.2, 129.9, 129.7, 128.4, 127.4, 127.3, 127.1, 126.5, 125.4, 124.0, 123.5, 122.1, 121.0, 120.8, 120.6, 120.0, 119.8, 119.7, 119.1, 115.4 (Ar-CH, Ar-C), 55.4 (*N*-CH), 36.2, 36.1 (C–CH_3), 32.4, 32.3 (CH_3) 31.8, 30.0, 26.9, 22.8 (CH_2) 14.4 (CH_3) ppm; MS (MALDI-TOF, dctb): m/z = 1577.8 (100 %, $C_{108}H_{100}N_6O_6$ $[M]^+$); HRMS: (MALDI-TOF, dctb): calculated for ($C_{108}H_{100}N_6O_6$ $[M]^+$) m/z = 1576.7699, found m/z = 1576.7696; UV/Vis (CH_2Cl_2): λ [nm] (ε [L mol^{-1} cm^{-1}]) = 372 (54 000), 571 (11 100).

Acknowledgements

The authors thank the Deutsche Forschungsgemeinschaft (DFG–SFB 953 „Synthetic Carbon Allotropes“, and the Graduate School Molecular Science (GSMS) for financial support. Open access funding enabled and organized by Projekt DEAL.

Conflict of interest

The authors declare no conflict of interest.

Keywords: chirality · helicene · hexabenzocoronene · naphthalene · π-extension

[1] a) K. Y. Cheung, C. K. Chan, Z. Liu, Q. Miao, *Angew. Chem. Int. Ed.* **2017**, *56*, 9003 – 9007; *Angew. Chem.* **2017**, *129*, 9131 – 9135; b) J. M. Fernández-García, P. J. Evans, S. Medina Rivero, I. Fernández, D. García-Fresnadillo, J. Perles, J. Casado, N. Martín, *J. Am. Chem. Soc.* **2018**, *140*, 17188 – 17196; c) J. Ma, K. Zhang, K. S. Schellhammer, Y. Fu, H. Komber, C. Xu, A. A. Popov, F. Hennersdorf, J. J. Weigand, S. Zhou, W. Pisula, F. Ortmann, R. Berger, J. Liu, X. Feng, *Chem. Sci.* **2019**, *10*, 4025 – 4031; d) M. A. Majewski, M. Stępień, *Angew. Chem. Int. Ed.* **2019**, *58*, 86 – 116; *Angew. Chem.* **2019**, *131*, 90 – 122; e) I. R. Márquez, S. Castro-Fernández, A. Millán, A. G. Campaña, *Chem. Commun.* **2018**, *54*, 6705 – 6718; f) S. H. Pun, Q. Miao, *Acc. Chem. Res.* **2018**, *51*, 1630 – 1642; g) S. H. Pun, Y. Wang, M. Chu, C. K. Chan, Y. Li, Z. Liu, Q. Miao, *J. Am. Chem. Soc.* **2019**, *141*, 9680 – 9686; h) Y. Zhu, X. Guo, Y. Li, J. Wang, *J. Am. Chem. Soc.* **2019**, *141*, 5511 – 5517.

[2] J. Meisenheimer, K. Witte, *Ber. Dtsch. Chem. Ges.* **1903**, *36*, 4153 – 4164.

[3] a) H. Wynberg, *Acc. Chem. Res.* **1971**, *4*, 65 – 73; b) R. H. Martin, *Angew. Chem. Int. Ed. Engl.* **1974**, *13*, 649 – 660; *Angew. Chem.* **1974**, *86*, 727 – 738; c) W. H. Laarhoven, W. J. C. Prinsen in *Stereochemistry, Topics in Current Chemistry*; (Ed. W. H. Laarhoven), Springer-Verlag, Berlin, **1994**, pp. 63 – 130; d) L. Liu, T. J. Katz, *Tetrahedron Lett.* **1990**, *31*, 3983 – 3986; e) M. Gingras, *Chem. Soc. Rev.* **2013**, *42*, 968 – 1006; f) M. Gingras, G. Félix, R. Peresutti, *Chem. Soc. Rev.* **2013**, *42*, 1007 – 1050; g) M. Gingras, *Chem. Soc. Rev.* **2013**, *42*, 1051 – 1095; h) Y. Shen, C.-F. Chen, *Chem. Rev.* **2012**, *112*, 1463 – 1535.

[4] a) Y. Yang, R. C. da Costa, M. J. Fuchter, A. J. Campbell, *Nat. Photonics* **2013**, *7*, 634 – 638; b) W. S. Brickell, A. Brown, C. M. Kemp, S. F. Mason, *J. Chem. Soc. A* **1971**, *0*, 756 – 760; c) M. S. Newman, D. Lednicer, *J. Am. Chem. Soc.* **1956**, *78*, 4765 – 4770.

[5] a) B. J. Coe, D. Rusanova, V. D. Joshi, S. Sánchez, J. Vávra, D. Khobragade, L. Severa, I. Císařová, D. Šaman, R. Pohl, K. Clays, G. Depotter, B. S. Brunschwig, F. Teplý, *J. Org. Chem.* **2016**, *81*, 1912 – 1920; b) K. Clays, K. Wostyn, A. Persoons, S. Maiorana, A. Papagni, C. A. Daul, V. Weber, *Chem. Phys. Lett.* **2003**, *372*, 438 – 442; c) T. Verbiest, S. van Elshocht, M. Kauranen, L. Hellemans, J. Snauwaert, C. Nuckolls, T. Katz, A. Persoons, *Science* **1998**, *282*, 913 – 915.

[6] a) K. Yavari, P. Aillard, Y. Zhang, F. Nuter, P. Retailleau, A. Voituriez, A. Marinetti, *Angew. Chem. Int. Ed.* **2014**, *53*, 861 – 865; *Angew. Chem.* **2014**, *126*, 880 – 884; b) P. Aillard, D. Dova, V. Magné, P. Retailleau, S. Cauteruccio, E. Licandro, A. Voituriez, A. Marinetti, *Chem. Commun.* **2016**, *52*, 10984 – 10987; c) Z. Krausová, P. Sehnal, B. P. Bondzic, S. Chercheja, P. Eilbracht, I. G. Stará, D. Šaman, I. Starý, *Eur. J. Org. Chem.* **2011**, 3849 – 3857.

[7] a) E. Anger, M. Srebro, N. Vanthuyne, L. Toupet, S. Rigaut, C. Roussel, J. Autschbach, J. Crassous, R. Réau, *J. Am. Chem. Soc.* **2012**, *134*, 15628 – 15631; b) B. L. Feringa, N. P. M. Huck, A. M. Schoevaars, *Adv. Mater.* **1996**, *8*, 681 – 684; c) C. Shen, G.'h. Loas, M. Srebro-Hooper, N. Vanthuyne, L. Toupet, O. Cador, F. Paul, J. T. López Navarrete, F. J. Ramírez, B. Nieto-Ortega, J. Casado, J. Autschbach, M. Vallet, J. Crassous, *Angew. Chem. Int. Ed.* **2016**, *55*, 8062 – 8066; *Angew. Chem.* **2016**, *128*, 8194 – 8198; d) D. Schweinfurth, M. Zalibera, M. Kathan, C. Shen, M. Mazzolini, N. Trapp, J. Crassous, G. Gescheidt, F. Diederich, *J. Am. Chem. Soc.* **2014**, *136*, 13045 – 13052.

[8] a) G. Lewińska, K. S. Danel, J. Sanetra, *Sol. Energy* **2016**, *135*, 848 – 853; b) L. Shan, D. Liu, H. Li, X. Xu, B. Shan, J.-B. Xu, Q. Miao, *Adv. Mater.* **2015**, *27*, 3418 – 3423; c) S. Xiao, M. Myers, Q. Miao, S. Sanaur, K. Pang, M. L. Steigerwald, C. Nuckolls, *Angew. Chem. Int. Ed.* **2005**, *44*, 7390 – 7394; *Angew. Chem.* **2005**, *117*, 7556 – 7560; d) Y. Yang, L. Yuan, B. Shan, Z. Liu, Q. Miao, *Chem. Eur. J.* **2016**, *22*, 18620 – 18627.

[9] a) T. Otani, A. Tsuyuki, T. Iwachi, S. Someya, K. Tateno, H. Kawai, T. Saito, K. S. Kanyiva, T. Shibata, *Angew. Chem. Int. Ed.* **2017**, *56*, 3906 – 3910; *Angew. Chem.* **2017**, *129*, 3964 – 3968; b) N. Saleh, B. Moore, M. Srebro, N. Vanthuyne, L. Toupet, J. A. G. Williams, C. Roussel, K. K. Deol, G. Muller, J. Autschbach, J. Crassous, *Chem. Eur. J.* **2015**, *21*, 1673 – 1681; c) J. Torras, O. Bertran, C. Alemán, *J. Phys. Chem. B* **2009**, *113*, 15196 – 15203; d) K. E. Phillips, T. J. Katz, S. Jockusch, A. J. Lovinger, N. J. Turro, *J. Am. Chem. Soc.* **2001**, *123*, 11899 – 11907; e) J. E. Field, G. Muller, J. P. Riehl, D. Venkataraman, *J. Am. Chem. Soc.* **2003**, *125*, 11808 – 11809; f) F. Dumitrascu, D. G. Dumitrascu, I. Aron, *Arkivoc* **2010**, 1 – 32; g) A. V. Gulevskaya, E. A. Shvydkova, D. I. Tonkoglazova, *Eur. J. Org. Chem.* **2018**, 5030 – 5043.

[10] a) Y. Nakakuki, T. Hirose, H. Sotome, H. Miyasaka, K. Matsuda, *J. Am. Chem. Soc.* **2018**, *140*, 4317 – 4326; b) T. Hatakeyama, S. Hashimoto, T. Oba, M. Nakamura, *J. Am. Chem. Soc.* **2012**, *134*, 19600 – 19603; c) G. Treboux, P. Lapstun, Z. Wu, K. Silverbrook, *Chem. Phys. Lett.* **1999**, *301*, 493 – 497.

[11] a) T. Caronna, R. Sinisi, L. Malpezzi, S. V. Meille, A. Mele, M. Catellani, *Chem. Commun.* **2000**, 1139 – 1140; b) S. Han, D. R. Anderson, A. D. Bond, H. V. Chu, R. L. Disch, D. Holmes, J. M. Schulman, S. J. Teat, K. P. Vollhardt, G. D. Whitener, *Angew. Chem. Int. Ed.* **2002**, *41*, 3227 – 3230; *Angew. Chem.* **2002**, *114*, 3361 – 3364; c) R. H Martin, M. Baes, *Tetrahedron* **1975**, *31*, 2135 – 2137; d) R. H. Martin, G. Morren, J. J. Schurter, *Tetrahedron Lett.* **1969**, *10*, 3683 – 3688; e) M. Miyasaka, A. Rajca, M. Pink, S. Rajca, *J. Am. Chem. Soc.* **2005**, *127*, 13806 – 13807; f) A. Moradpour, H. Kagan, M. Baes, G. Morren, R. H. Martin, *Tetrahedron* **1975**, *31*, 2139 – 2143..

[12] a) T. Fujikawa, Y. Segawa, K. Itami, *J. Am. Chem. Soc.* **2015**, *137*, 7763 – 7768; b) Y. Hu, X.-Y. Wang, P.-X. Peng, X.-C. Wang, X.-Y. Cao, X. Feng, K. Müllen, A. Narita, *Angew. Chem.* **2017**, *129*, 3423 – 3427.

[13] a) G. Liu, T. Koch, Y. Li, N. L. Doltsinis, Z. Wang, *Angew. Chem. Int. Ed.* **2019**, *58*, 178 – 183; *Angew. Chem.* **2019**, *131*, 184 – 189; b) N. J. Schuster, R. Hernández Sánchez, D. Bukharina, N. A. Kotov, N. Berova, F. Ng, M. L. Steigerwald, C. Nuckolls, *J. Am. Chem. Soc.* **2018**, *140*, 6235 – 6239;

c) N. J. Schuster, D. W. Paley, S. Jockusch, F. Ng, M. L. Steigerwald, C. Nuckolls, *Angew. Chem. Int. Ed.* **2016**, *55*, 13519 – 13523; *Angew. Chem.* **2016**, *128*, 13717 – 13721; d) B. Liu, M. Böckmann, W. Jiang, N. L. Doltsinis, Z. Wang, *J. Am. Chem. Soc.* **2020**, *142*, 7092 – 7099; e) A. Hirsch, C. Weiss, D. Sharapa, *Chem. Eur. J.* **2020**, https://doi.org/10.1002/chem.202001703.

[14] a) M. Buchta, J. Rybáček, A. Jančařík, A. A. Kudale, M. Buděšínský, J. V. Chocholoušová, J. Vacek, L. Bednárová, I. Císařová, G. J. Bodwell, I. Starý, I. G. Stará, *Chem. Eur. J.* **2015**, *21*, 8910 – 8917; b) A.-C. Bédard, A. Vlassova, A. C. Hernandez-Perez, A. Bessette, G. S. Hanan, M. A. Heuft, S. K. Collins, *Chem. Eur. J.* **2013**, *19*, 16295 – 16302; c) Y. Hu, G. M. Paternò, X.-Y. Wang, X.-C. Wang, M. Guizzardi, Q. Chen, D. Schollmeyer, X.-Y. Cao, G. Cerullo, F. Scotognella, K. Müllen, A. Narita, *J. Am. Chem. Soc.* **2019**, *141*, 12797 – 12803.

[15] a) D. Reger, P. Haines, F. W. Heinemann, D. M. Guldi, N. Jux, *Angew. Chem. Int. Ed.* **2018**, *57*, 5938 – 5942; *Angew. Chem.* **2018**, *130*, 6044 – 6049; b) C. M. Cruz, S. Castro-Fernández, E. Maçôas, J. M. Cuerva, A. G. Campaña, *Angew. Chem. Int. Ed.* **2018**, *57*, 14782 – 14786; *Angew. Chem.* **2018**, *130*, 14998 – 15002; c) C. M. Cruz, S. Castro-Fernández, E. Maçôas, A. Millán, A. G. Campaña, *Synlett* **2019**, *30*, 997 – 1002; d) Y. Wang, Z. Yin, Y. Zhu, J. Gu, Y. Li, J. Wang, *Angew. Chem. Int. Ed.* **2019**, *58*, 587 – 591; *Angew. Chem.* **2019**, *131*, 597 – 601; e) P. J. Evans, J. Ouyang, L. Favereau, J. Crassous, I. Fernández, J. Perles, N. Martín, *Angew. Chem. Int. Ed.* **2018**, *57*, 6774 – 6779; *Angew. Chem.* **2018**, *130*, 6890 – 6895; f) N. Jux, M. M. Martin, F. Hampel, *Chem. Eur. J.* **2020**, *26*, 10210 – 10212.

[16] a) K. Kawasumi, Q. Zhang, Y. Segawa, L. T. Scott, K. Itami, *Nat. chem.* **2013**, *5*, 739 – 744; b) F. Schlütter, T. Nishiuchi, V. Enkelmann, K. Müllen, *Angew. Chem. Int. Ed.* **2014**, *53*, 1538 – 1542; *Angew. Chem.* **2014**, *126*, 1564 – 1568; c) S. Xiao, S. J. Kang, Y. Wu, S. Ahn, J. B. Kim, Y.-L. Loo, T. Siegrist, M. L. Steigerwald, H. Li, C. Nuckolls, *Chem. Sci.* **2013**, *4*, 2018.

[17] a) V. Coropceanu, J. Cornil, D. A. da Silva Filho, Y. Olivier, R. Silbey, J.-L. Brédas, *Chem. Rev.* **2007**, *107*, 926 – 952; b) A. Saeki, Y. Koizumi, T. Aida, S. Seki, *Acc. Chem. Res.* **2012**, *45*, 1193 – 1202; c) J.-L. Brédas, D. Beljonne, V. Coropceanu, J. Cornil, *Chem. Rev.* **2004**, *104*, 4971 – 5004.

[18] R. Rieger, K. Müllen, *J. Phys. Org. Chem.* **2010**, *23*, 315 – 325.

[19] a) S. V. Bhosale, C. H. Jani, S. J. Langford, *Chem. Soc. rev.* **2008**, *37*, 331 – 342; b) T. Weil, T. Vosch, J. Hofkens, K. Peneva, K. Müllen, *Angew. Chem. Int. Ed.* **2010**, *49*, 9068 – 9093; *Angew. Chem.* **2010**, *122*, 9252 – 9278.

[20] a) T. Khotavivattana, S. Calderwood, S. Verhoog, L. Pfeifer, S. Preshlock, N. Vasdev, T. L. Collier, V. Gouverneur, *Org. Lett.* **2017**, *19*, 568 – 571; b) J. Passays, C. Rubay, L. Marcélis, B. Elias, *Eur. J. Inorg. Chem.* **2017**, 623 – 629; c) L. Wang, X. Yang, X. Wang, L. Sun, *Dyes Pigm.* **2015**, *113*, 581 – 587; d) A. C. Krueger, W. M. Kati, W. A. Carroll, J. K. Pratt, D. K. Hutchinson, US 2012/0172290 Al; preparation of proline derivatives as antiviral agents useful in the treatment of HCV infection.

[21] P. Prasad, I. Khan, P. Kondaiah, A. R. Chakravarty, *Chem. Eur. J.* **2013**, *19*, 17445 – 17455.

[22] J. R. Johansson, Y. Wang, M. P. Eng, N. Kann, P. Lincoln, J. Andersson, *Chem. Eur. J.* **2013**, *19*, 6246 – 6256.

[23] M. M. Martin, D. Lungerich, P. Haines, F. Hampel, N. Jux, *Angew. Chem. Int. Ed.* **2019**, *58*, 8932 – 8937; *Angew. Chem.* **2019**, *131*, 9027 – 9032.

[24] S. Ehrlich, H. F. Bettinger, S. Grimme, *Angew. Chem. Int. Ed.* **2013**, *52*, 10892 – 10895; *Angew. Chem.* **2013**, *125*, 11092 – 11096.

[25] G. M. Upadhyay, H. R. Talele, S. Sahoo, A. V. Bedekar, *Tetrahedron Lett.* **2014**, *55*, 5394 – 5399.

Manuscript received: July 20, 2020
Revised manuscript received: August 14, 2020
Accepted manuscript online: August 20, 2020
Version of record online: November 30, 2020